

RADIAL FOCUSING IN AN INDUCTION LINAC GAP\*

Yinbao Chen† and M. Reiser  
 Laboratory for Plasma Research  
 University of Maryland, College Park, MD 20742

ABSTRACT

The focusing properties of the electric field distribution in an induction linac gap are identical to those of a bipotential electrostatic lens if the particle gap-transit time is small compared with the time variation of the induced electric field. Bipotential lenses have been studied systematically only in the nonrelativistic case. In this paper we present the results of a theoretical study of the focusing properties of a symmetrical two-cylinder lens with identical radii and negligible separation for relativistic electron beams. Analytical formulas derived by using the thin-lens approximation are compared with the results of numerical integration of the relativistic paraxial ray equation and found to be sufficiently accurate for practical applications.

INTRODUCTION

Two coaxial cylindrical electrodes with radius  $b$ , axial separation  $d$ , and with an electrostatic potential difference  $\Delta V = V_2 - V_1$  form an acceleration (or deceleration) gap in which particles with charge  $q$  gain (or lose) kinetic energy by an amount  $q\Delta V$ . Such a gap configuration, shown in Fig. 1, is also known as a bipotential lens since it produces a net focusing force on the traversing particles regardless of whether they gain or lose energy. The ion-optical properties of such a lens are well known for nonrelativistic particle energies; detailed calculations and tables of the lens parameters can be found, for instance, in the book by El Karch.<sup>1</sup>

In this paper we extend the existing first-order (paraxial) theory of the bipotential lens to the relativistic regime. Using the thin-lens approximation we find analytic formulas for the focal lengths  $f_1, f_2$  for the case when the gap width is small compared to the radius of the electrodes ( $d \ll b$ ). The analytical results are compared to numerical integration, and excellent agreement (better than 7%) is found in all cases considered.

Our results are of particular interest to single-gap high-voltage electrostatic acceleration systems and induction linacs for electron beams. Induction linacs are being used successfully for free electron lasers (FELs),<sup>2</sup> as injectors for relativistic klystrons,<sup>3</sup> and in many other experiments with intense relativistic electron beams. The accelerating gap voltage in such a linac is being produced by a time varying azimuthal magnetic field, and from Faraday's law one finds

$$\Delta V = V_2 - V_1 = \frac{\partial \Psi}{\partial t}, \quad (1)$$

where  $\Psi = \int B_\theta dr dz$  is the azimuthal magnetic flux around the gap. If the flux changes linearly with time by an amount  $\Psi_1$  during a time interval  $\tau$ , i.e. if  $\Psi(t) = \Psi_0 + \Psi_1 t/\tau$ , then the voltage across the gap is given, according to (1), by

$$\Delta V = V_2 - V_1 = \frac{\Psi_1}{\tau} = \text{const.} \quad \text{for } 0 \leq t \leq \tau. \quad (2)$$

Thus, for electrons crossing the gap during the time interval  $\tau$  the effect of the induced electric field is practically identical

with that of an equivalent electrostatic field. For typical parameters like  $b = 2 - 10 \text{ cm}$ ,  $V \geq 100 \text{ kV}$ , and  $\tau = 10 - 100 \text{ ns}$ , electron transit times in the gap are of the order of a nanosecond or less; hence this electrostatic equivalence criterion is well satisfied. When the flux change with time is nonlinear, e.g.,  $\Psi(t) = \Psi_0 + \Psi_1(t/\tau)^2$ , the electrostatic equivalence criterion is still satisfied as long as the gap transit time is negligibly small compared to the time  $\tau$ . However, in this case the voltage across the gap, and hence the particle energy gain as well as the radial focusing effect, will depend on the time  $t$  when the particle traverses the gap.

The potential distribution for a bipotential lens, as illustrated in Fig. 1, can be found by solving Laplace's equation and has the general form<sup>1</sup>

$$\phi(r, z) = \frac{1}{2\pi} \int_{-\infty}^{\infty} a_k(k) J_0(ikr) e^{ikz} dk, \quad (3)$$

where  $J_0(ikr)$  is the normal Bessel function of the first kind of zero order and the coefficients  $a_k(k)$  must be determined from the boundary conditions for  $\phi(r, z)$ . For the special case where the two cylinders have the same radius  $b$  and their separation is negligibly small (i.e.,  $d \ll b$ ), the potential function may be written in the form

$$\phi(r, z) = \frac{V_1 + V_2}{2} + \frac{V_2 - V_1}{\pi} \int_0^\infty \frac{\sin kz}{k} \frac{J_0(ikr)}{J_0(ikb)} dk \quad (4)$$

where  $V_1$  and  $V_2$  are the potentials corresponding to the electron energies before and after the gap traversal, respectively, and  $\Delta V = V_2 - V_1$  is the potential difference across the gap.

The potential variation  $\phi(0, z) = V(z)$  along the axis and the first two derivatives,  $V'(z) = dV/dz$  and  $V''(z) = d^2V/dz^2$ , are shown in Fig. 2. Note that for convenience of plotting we set  $V_1 = 0$  and  $V_2 = 1$ . This variation can be approximated with a good degree of accuracy by the expression<sup>1</sup>

$$\phi(0, z) = V(z) = \frac{V_1 + V_2}{2} + \frac{V_2 - V_1}{2} \tanh \alpha z, \quad (5)$$

where  $\alpha = 1.32/b$ . The two derivative functions are then:

$$V'(z) = \frac{V_2 - V_1}{2} \alpha (1 - \tanh^2 \alpha z); \quad (6)$$

$$V''(z) = \alpha^2 (V_2 - V_1) (\tanh^3 \alpha z - \tanh \alpha z); \quad (7)$$

RELATIVISTIC PARAXIAL RAY EQUATION

The relativistically correct paraxial ray equation for an axially symmetric electrostatic focusing system with no magnetic lenses and for particles with zero canonical angular momentum  $p_\theta$  can be written as<sup>4</sup>

$$r'' + \frac{\gamma'}{\beta^2 \gamma} r' + \frac{\gamma''}{2\beta^2 \gamma} r = 0. \quad (8)$$

In this equation,  $r = r(z)$  is the radius of the particle trajectory,  $' = d/dz$ ,  $\beta = v/c$  is the ratio of the particle velocity,  $v$ , to the speed of light,  $c$ , and  $\gamma = (1 - \beta^2)^{-1/2}$  is the relativistic mass factor defined in terms of the potential function  $V(z)$  as

$$\gamma = 1 + \frac{qV(z)}{m_0 c^2}. \quad (9)$$

\*Research supported by U.S. Department of Energy.

†Permanent address: Institute of Atomic Energy Beijing, People's Republic of China.

Equation (8) can be rewritten as

$$r'' + g_1 r' + g_2 r = 0, \quad (10)$$

with  $g_1 = \gamma'/\beta^2\gamma$  and  $g_2 = \gamma''/2\beta^2\gamma$ .

The term  $g_1 r'$  in Eq. (10) can be eliminated by introducing the "reduced" variable

$$R(z) = r(z)(\gamma^2 - 1)^{1/4}, \quad (11)$$

which results in the equation

$$R''(z) + G(z)R(z) = 0, \quad (12)$$

where

$$G = g_2 - \frac{1}{4}g_1^2 - \frac{1}{2}g_1' = \frac{\gamma'^2(1 + \frac{1}{2}\gamma^2)}{2(\gamma^2 - 1)^2}. \quad (13)$$

In the nonrelativistic limit, one can use the approximations

$$\gamma^2 \approx 1 + \frac{2qV}{m_0c^2}, \quad (14)$$

$$\gamma'^2 \approx \left(\frac{q}{m_0c^2}\right)^2 V'^2, \quad (15)$$

and obtains from Eq. (13) the results

$$G = \frac{3}{16} \frac{V'^2}{V^2}. \quad (16)$$

### THIN-LENS APPROXIMATION

Equation (12) can be integrated if one uses the thin-lens approximation in which the reduced particle radius in the gap region is assumed to be constant; the change of the slope due to the lens action is then given by

$$R_2' - R_1' = - \int_{z_1}^{z_2} G(z)R(z)dz = -\bar{R} \int_{z_1}^{z_2} G(z)dz, \quad (17)$$

where  $z_1$  and  $z_2$  define the axial width of the gap field and  $R(z) = \bar{R} = \text{const}$  in the gap region, as stated.

From Eq. (5) and Eq. (9) one gets

$$\begin{aligned} \gamma^2 &= \left[1 + \frac{q}{m_0c^2} \left(\frac{V_1 + V_2}{2} + \frac{V_2 - V_1}{2} \tanh \alpha z\right)\right]^2 \\ &= 1 + C + B\xi + A\xi^2 \\ &= 1 + D, \end{aligned} \quad (18)$$

where

$$\xi = \tanh \alpha z; \quad (19)$$

$$C = \left(\frac{q}{m_0c^2} \frac{V_1 + V_2}{2}\right)^2 + \frac{q}{m_0c^2}(V_1 + V_2); \quad (20)$$

$$B = \frac{q}{m_0c^2}(V_2 - V_1) \left[1 + \frac{1}{2} \frac{q}{m_0c^2}(V_1 + V_2)\right]; \quad (21)$$

$$A = \left(\frac{q}{m_0c^2} \frac{V_2 - V_1}{2}\right)^2; \quad (22)$$

and

$$D = A\xi^2 + B\xi + C. \quad (23)$$

Also from Eq. (6), one obtains

$$\gamma'^2 = A\alpha^2(1 - \xi^2)^2. \quad (24)$$

Substitution of Eq. (18) and Eq. (24) into the Eq. (13), yields

$$G = \frac{A\alpha^2}{4} \left[ \frac{3(1 - \xi^2)^2}{D^2} + \frac{(1 - \xi^2)^2}{D} \right]. \quad (25)$$

Therefore, the integral in Eq. (17) becomes

$$\int_{z_1}^{z_2} G(z)dz = \frac{A\alpha}{4} \int_{-1}^1 \left[ \frac{3(1 - \xi^2)}{D^2} + \frac{1 - \xi^2}{D} \right] d\xi. \quad (26)$$

Here the limits of the integration are assumed to be outside the field region, i.e., we can take  $z_1 \rightarrow -\infty$ ,  $z_2 \rightarrow \infty$ , so that

$$\begin{aligned} \tanh \alpha z_1 &= -1, \quad \gamma = \gamma_1 = 1 + qV_1/m_0c^2, \quad \gamma_1' = 0, \\ \tanh \alpha z_2 &= 1, \quad \gamma = \gamma_2 = 1 + qV_2/m_0c^2, \quad \gamma_2' = 0. \end{aligned} \quad (27)$$

The integral (26) can be solved analytically, and one obtains for the change of the slope by substitution into Eq. (17)

$$\begin{aligned} R_2' - R_1' &= - \frac{\alpha \bar{R}}{4} \left[ \frac{\gamma_1 + \gamma_2 + \frac{1}{2}(\gamma_1\gamma_2 - 5)}{\gamma_2 - \gamma_1} \log \frac{\gamma_2^2 - 1}{\gamma_1^2 - 1} \right. \\ &\quad \left. - \frac{\gamma_1\gamma_2 - 5}{\gamma_2 - \gamma_1} \log \frac{\gamma_2 + 1}{\gamma_1 + 1} - 5 \right]. \end{aligned} \quad (28)$$

From the definition (11) one gets for the actual radius on either side of the lens

$$r_1 = \frac{R_1}{(\gamma_1^2 - 1)^{1/4}}, \quad r_2 = \frac{R_2}{(\gamma_2^2 - 1)^{1/4}}. \quad (29)$$

The focal length  $f_2$  on the downstream (image) side of the lens is defined by a particle entering the lens with initial slope  $r_1' = 0$  and radius  $r_1$ . If the slope after passage through the lens is  $r_2'$ , we have  $f_2 = -r_1/r_2'$ . Assuming that  $\bar{R} = R_1$ , we obtain in view of (29) the relation

$$\begin{aligned} \frac{1}{f_2} &= \frac{\alpha}{4} \left(\frac{\gamma_1^2 - 1}{\gamma_2^2 - 1}\right)^{1/4} \left[ \frac{\gamma_1 + \gamma_2 + \frac{1}{2}(\gamma_1\gamma_2 - 5)}{\gamma_2 - \gamma_1} \log \frac{\gamma_2^2 - 1}{\gamma_1^2 - 1} \right. \\ &\quad \left. - \frac{\gamma_1\gamma_2 - 5}{\gamma_2 - \gamma_1} \log \frac{\gamma_2 + 1}{\gamma_1 + 1} - 5 \right]. \end{aligned} \quad (30)$$

The focal length  $f_1$  on the upstream (object) side of the lens is then determined by the well-known relation between focal length  $f$  and momentum  $p$  on each side of the lens, namely  $f_2/f_1 = p_2/p_1 = (\gamma_2^2 - 1)^{1/2}/(\gamma_1^2 - 1)^{1/2}$ . Hence,

$$\begin{aligned} \frac{1}{f_1} &= \frac{\alpha}{4} \left(\frac{\gamma_2^2 - 1}{\gamma_1^2 - 1}\right)^{1/4} \left[ \frac{\gamma_1 + \gamma_2 + \frac{1}{2}(\gamma_1\gamma_2 - 5)}{\gamma_2 - \gamma_1} \log \frac{\gamma_2^2 - 1}{\gamma_1^2 - 1} \right. \\ &\quad \left. - \frac{\gamma_1\gamma_2 - 5}{\gamma_2 - \gamma_1} \log \frac{\gamma_2 + 1}{\gamma_1 + 1} - 5 \right]. \end{aligned} \quad (31)$$

In the nonrelativistic limit, Eq. (30) becomes

$$\frac{1}{f_2} = \frac{3}{8} \alpha \left(\frac{V_1}{V_2}\right)^{1/4} \left[ \frac{V_1 + V_2}{V_2 - V_1} \log \frac{V_2}{V_1} - 2 \right] \quad (32)$$

which agrees with the formula in Reference 1.

### COMPUTATIONAL RESULTS

To check the accuracy of the thin-lens approximation used in deriving the analytical relations (30) to (32) for the focal lengths we integrated Eq. (8) numerically. The action of a lens can be represented by the well-known matrix equation

$$\begin{pmatrix} r_2 \\ r_2' \end{pmatrix} = \begin{bmatrix} 1 - d_2/f_2 & f_1(d_1/f_1 + d_2/f_2 - d_1d_2/f_1f_2) \\ -1/f_2 & (f_1/f_2)(1 - d_1/f_1) \end{bmatrix} \begin{pmatrix} r_1 \\ r_1' \end{pmatrix}, \quad (33)$$

which relates the projected radius and slope of the outgoing trajectory  $(r_2, r_2')$  at the lens center to  $(r_1, r_1')$  of the incoming trajectory. The parameters  $d_1$  and  $d_2$  measure the distance of the two principal planes I and II, respectively, from the center of the lens. They are both positive quantities if plane I is downstream (image side) and plane II is upstream (object side) of the lens center.

The results of the numerical integration for different voltages  $V_1$  and  $V_2$  are tabulated in Table 1. Note that  $d_1$  is negative and  $d_2$  is positive which implies that both principle planes

are on the upstream side of the gap center.

In Table 2 we compare the analytical results for  $b/f_2$  from Eq. (30) with the numerical data. The accuracy of the analytical formula is seen to be in the range of a few percent which is adequate for most practical purposes.

Finally, in Fig. 3 we plotted  $b/f_2$  versus  $V_2/V_1$  for different relativistic values of the initial electron voltage  $V_1$ , and for the nonrelativistic (NR) energy regime using the analytical formulas (30) and (32). For completeness, we included the cases where  $V_2 < V_1$ , i.e. where the gap has a decelerating field polarity. We note from this figure that the nonrelativistic formula overestimates the focusing strength  $b/f_2$  when the gap is accelerating. But, surprisingly, there is no difference between relativistic and nonrelativistic energies when the gap voltage is decelerating the electrons ( $V_2/V_1 < 1$ ).

Finally, we would like to note that the nonrelativistic results are also of interest to induction linacs for ions such as accelerator experiments for heavy ion fusion.<sup>5</sup>

REFERENCES

1. A.B. El-Kareh and J.C.J. El-Kareh, *Electron Beams, Lenses, and Optics*, vol. 1, Academic Press, New York and London, 1970.
2. T.J. Orzechowski, et al., *Phys. Rev. Lett.*, **54**, 889 (1985).
3. A.M. Sessler, S.S. Yu, *Phys. Rev. Lett.*, **58**, 2439 (1987).
4. J.D. Lawson, *The Physics of Charged-Particle Beams*, Oxford University Press, 1977.
5. D. Keefe, AIP Conf. Proc. *Heavy Ion Fusion* (Editors: M. Reiser, T. Godlove, and R. Bangertner), Vol. 152, p. 63 (1986).

Table 1. Numerical results for lens parameters for different electron beam voltages  $V_1$  and  $V_2$  before and after gap crossing.

$V_1$ (kV)	$V_2$ (kV)	$b/f_2$	$d_2/f_2$	$b/f_1$	$-d_1/f_1$
100	200	.0296	.159	.0442	.198
	300	.0624	.258	.1183	.355
	400	.0893	.316	.1980	.485
200	300	.0112	.104	.0142	.117
	400	.0274	.194	.0434	.214
	500	.0442	.236	.0791	.304
300	400	.0057	.073	.0071	.086
	500	.0164	.138	.0227	.162
	600	.0279	.168	.0436	.228
500	600	.0024	.056	.0027	.057
	700	.0074	.096	.0097	.111
	800	.0141	.138	.0198	.161

Table 2. Comparison of analytical and numerical results.

$V_1$ (kV)	$V_2$ (kV)	$(b/f_2)$ anal.	$(b/f_2)$ num.	$\Delta$
100	200	.0302	.0296	.020
	300	.0658	.0624	.054
	400	.0941	.0893	.054
200	300	.0109	.0112	-.027
	400	.0288	.0274	.051
	500	.0463	.0442	.047
300	400	.0056	.0057	-.017
	500	.0163	.0164	-.006
	600	.0280	.0279	.004
500	600	.0023	.0024	-.041
	700	.0074	.0074	-.001
	800	.0138	.0141	-.021

$$\Delta = \frac{(b/f_2)_{anal.} - (b/f_2)_{num.}}{(b/f_2)_{num.}}$$

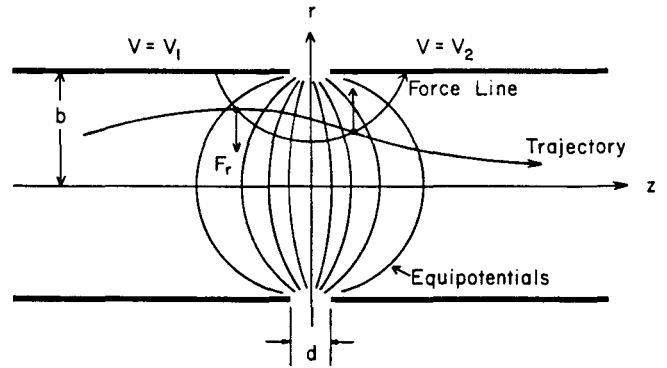


Fig. 1. Electric field configuration and trajectory (schematic) in an induction gap (electrostatic bipotential lens).

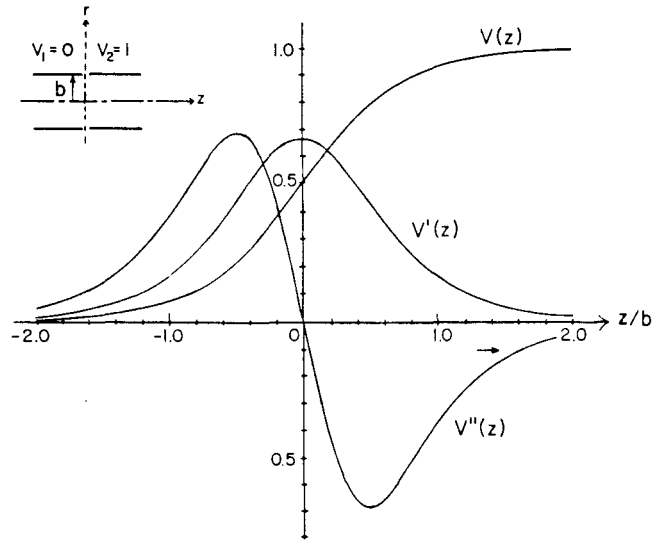


Fig. 2. Potential distribution  $V(z)$  and derivatives  $V'(z), V''(z)$  on the axis of the lens ( $r = 0$ ).

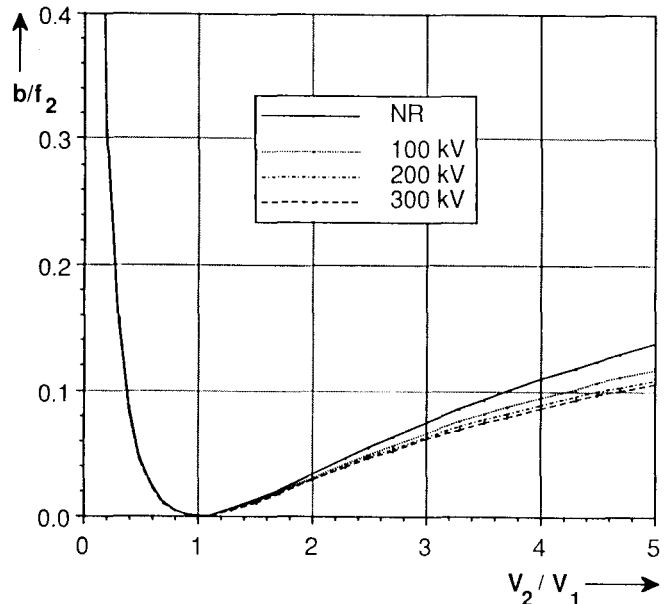


Fig. 3. Focusing strength  $b/f_2$  versus voltage ratio  $V_2/V_1$  for different relativistic electron beam voltages  $V_1$  and for the nonrelativistic regime (NR).